Journal of Digital Imaging

Quantitative Analysis of Three-dimensional Rendered Imaging of the Human Skull Acquired from Multi-Detector Row Computed Tomography

Haijo Jung, Hee-Joung Kim, Dong-Ook Kim, Soon-Il Hong, Ha-Kyu Jeong, Kee-Deog Kim, Yong Oock Kim, Sun Kook Yoo, and Hyung Sik Yoo

The purpose of this study was to evaluate the quantitative accuracy of three-dimensional (3D) rendered images acquired with multi-detector row computed tomography (MDCT) by means of distance measurements of a dry human skull for various slice thicknesses and acquisition modes. A radiologist directly measured the distance of line items on the skull surface to establish reference ''gold standards.'' The skull specimen was scanned with a MDCT with various scanning parameters (slice thicknesses and acquisition modes). An observer measured the corresponding distances of the same items on 3D rendered images. The quantitative accuracy of distance measurements was statistically evaluated. There were no significant statistical differences (*P* value <.05) in accuracy of distance measurements among the scan modes. However, the results showed that acquisition slice thickness was the influential factor in determining the accuracy of the 3D rendered MDCT images. The quantitative analysis of distance measurement may be a useful tool evaluating the accuracy and defining optimal parameters of 3D rendered images.

KEY WORDS: Multi-detector computed tomography (MDCT), 3D rendered image, skull specimen, scanning parameter, quantitative accuracy, distance measurement

INTRODUCTION

THE ADVENT of x-ray computed tomography (CT) in the early 1970s revolutionized the field of medical imaging by providing clinically useful information from a large number of cross-sectional images, an option not available with plain radiography. In the late 1980s, the introduction of helical (or spiral) CT dramatically improved the performance of continuous CT scanning over the axial CT of the step-and-shoot mode and led to dose reduction and shorter scanning time for the same volume coverage. In recent years, refinements in helical CT have led to the development of multi-detector row CT (MDCT), a system equipped with multiple detector banks, which offers relatively shorter acquisition times and increased longitudinal (z-axis) resolution.[1-4] For this reason, MDCT can acquire a large quantity of cross-sectional image data in a relatively short scanning time, which results in improved details in three-dimensional (3D) reconstruction and better visualization of anatomical structures. With the implementation of picture archiving communication system (PACS) in many hospitals, digital imaging data has become readily accessible. Further, the development of rendering techniques has enhanced the capability of displaying 3D imaging. The development of 3D visualization imaging medical software was based on high-performance computer workstations, but it has now developed to the point where such software can be based on a personal computer (PC) at a real-time rate.

From the Department of Radiology, College of Medicine, Yonsei University, Seoul, Korea; Research Institute of Radiological Science, Yonsei University, Seoul, Korea; BK21 Project for Medical Sciences, Yonsei University, Seoul, Korea; the Department of Dental Radiology, College of Dentistry, Yonsei University, Seoul, Korea; the Department of Plastic and Reconstructive Surgery, College of Medicine, Yonsei University, Seoul, Korea; and the Department of Medical Engineering, College of Medicine, Yonsei University, Seoul, Korea.

Correspondence to: Hee-Joung Kim, Associate Professor, Department of Diagnostic Radiology, College of Medicine, Yonsei University, 134 Shinchon-dong Seodaemoon-ku, Seoul 120-752, Korea; tel: 822-361-5753; fax: 822-313-1039; e-mail: hjkim@yumc.yonsei.ac.kr.

Online publication 21 January 2003

doi: 10.1007/s10278-002-0031-6

Therefore, CT image data coupled with a rendering technique have increased the range of possible medical applications for detailed 3D imaging and complicated spatial information. Three-dimensional rendered images may be perspectively visualized in any plane or projection using rotation and translation of the reconstructed image and by controlling within a suitable range of opacity. The potential applications for the information available from 3D rendered images have been rapidly increasing in the fields of diagnosis, and surgical or radiotherapy planning.[5-9]

In general, the image quality of tomographic or planer images has been evaluated quantitatively or qualitatively using appropriate phantoms or visual grading analysis. The image quality of 3D images has been widely investigated by the qualitative analysis method.[10-12] A need remains for an objective and quantitative method to assess the image quality of 3D rendered images.[13,14] In this study we mainly addressed the spatial accuracy of the model, which is one part of image quality; we presented the quantitative evaluation of 3D rendered images using bone reference points on a human skull phantom in comparison with direct distance measurements.

The purpose of this study was to evaluate the quantitative accuracy of 3D rendered images obtained with MDCT, scanned at various scanning parameters (scan modes and slice thicknesses). The direct distances measured on the skull phantom were analyzed statistically in comparison with corresponding projected distances measured on the 3D rendered MDCT images.

MATERIALS AND METHODS

Skull Specimen and Direct Distance Measurements

We prepared a human dried skull specimen to evaluate the quantitative accuracy of 3D rendered MDCT images. Twelve reference points, chosen for their important role on the craniofacial bone surface in plastic surgery and dentistry, were marked on the skull surface according to the description outlined in Table 1 and illustrated in Fig 1.[15]

Before CT scanning of the skull specimen, direct distance measurements of 21 lines between selected reference points were made, and each was repeated four times by a radiologist using a digital vernier caliper (Mitutoyo Co., Tokyo, Japan). Each measurement was recorded with an accuracy of 0.01 mm. The means of these five direct measurements were used as reference "gold standards" in this study for evaluation of the quantitative accuracy of 3D rendered CT images.

Image Acquisition Using MDCT

The skull specimen was immersed in a rectangular acrylic container of dimensions $23 \times 25 \times 23$ cm^3, filled with ordinary water to simulate the soft tissues of the head. The skull specimen was placed on the gantry table in the supine position, as in routine clinical practice, and was subsequently imaged with a MDCT scanner, that is used clinically for patients in Yonsei University Medical Center (YUMC).

The MDCT scans, using four-slice detector arrays, were performed under 12 different sets of conditions obtained by varying the parameters of slice thickness and scan mode as follows: slice thicknesses of 1.25, 2.50, 3.75, and 5.00 mm applied to a clinical protocol for different scan modes of axial scan, helical scan of high-quality mode (pitch of 0.75), and high-speed mode (pitch of 1.5).[4] Experimental acquisition parameters were tube rotation through 360° in 1 second in axial scan mode, 200 mA tube current, 120 kVp x-ray tube voltage, with a 22-cm display field of view (DFOV), a gantry angle of 0 degrees, and a 512×512 matrix. Imaging reconstruction parameters were reconstruction axial thickness the same as the scanning slice thickness and standard

Table 1. Reference Points on the Skull Surface for Distance Measurement

No.	Abbreviation	Name
1	A	Subspinale, Ss: most posterior point of maxillary bone
2	Ans	Spinal point, Sp: end point of anterior nasal spine
3	B	Supramentale, Sm: middle sagittal deepest point between pogonion and infradentale
4	Ba	Basion: anterior midpoint of foramen magnum
5	Co	Condylio, ed: most lateral point on the surface of the head of the mandible
6	Go	Gonion: most inferior, posterior, and lateral point on the angle of the mandible
7	Me	Medial point of the very middle suture
8	N	Nasion: medial point of frontal and nasal suture in midsagittal plane
9	Or	Orbitale: most base point of orbital bottom
10	Pns	Posterior nasal spine: most posterior point of maxillary bone
11	Pog	Pogonion: anterior midpoint of the chin
12	Zm	Zygomaxillary: lowest point on the suture between the zygomatic and maxillary bones

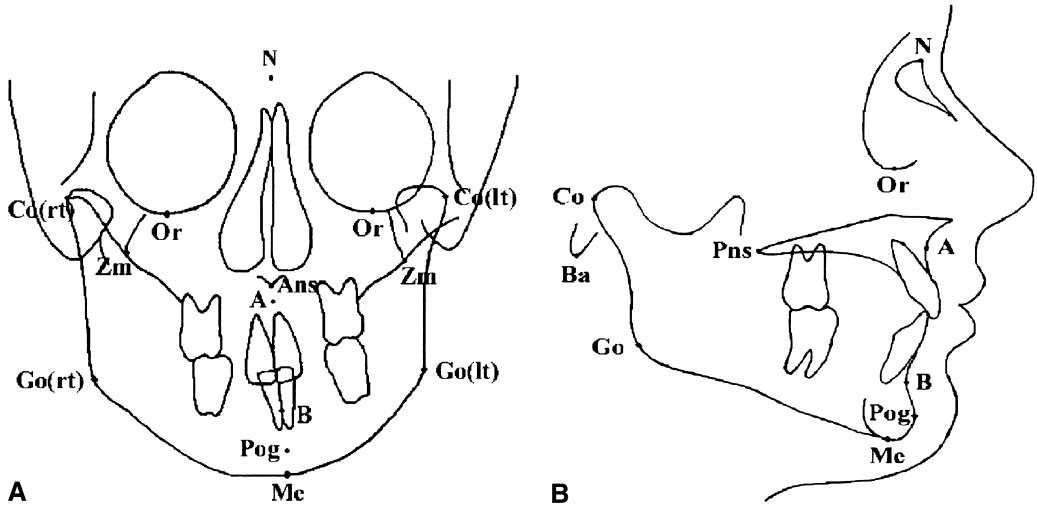

Fig 1. Front (a) and lateral (b) views of 12 reference points on the skull specimen.

reconstruction kernel for all examinations. In the helical mode, table speeds were applied from 3.75 mm to 15.00 mm per rotation to acquire the high-quality images available in the manufacturer's protocol. For each acquisition parameter and examination, total scanning time and number of reconstructed slices were recorded as shown in Table 2.

3D Image Reconstruction and Distance Measurements on 3D rendered images

The tomographic data reconstructed in the MDCT console were transferred in the digital image and communications in medicine (DICOM) image format to GE advantage workstation (AW) systems (GE Medical Systems, Milwaukee, WI) through a network for further processing or data saving. Then, 3D renderings were generated, and distance measurements were made on each 3D rendered image with a PC-based volumetric analysis tool, Vworks 4.0 (CyberMed Inc., Seoul, Korea).

Three-dimensional rendered images through shaped surface display (SSD) were displayed simultaneously on the user interface window with axial, coronal, and sagittal multi-planar reformatting (MPR) images of the skull MDCT data, which helped to localize some points accurately on the skull surface (Fig. 2). The surface for SSD was defined by the segmentation based on the threshold. The head protocol in Vworks 4.0, which contains the predefined threshold value optimized for the 3D rendering of the skull from CT data, was initially selected and then slightly modified through user interaction until some points marked on the 3D rendered skull surface were actually located at the boundary of the skull in all three MPR images together. In that case, the predefined threshold and the adjusted threshold values for signed 16 bit gray level were 171 and 165, respectively.

From the refined SSD and MPR images, users, accurately selected the reference points to measure each distances as described in Table 1 and illustrated in Fig. 1. For users, seven repeat measurements were made to reduce the inaccuracies introduced by manual operation.

Statistical Analysis

Statistical analysis was performed with the SAS software package (version 6.12; SAS Institute, Cary, NC). To evaluate the quantitative accuracy of distance measurements on 3D rendered images according to scanning parameters, the means of the direct measurements for 21 reference lines were

Table 2. Image Acquisition Parameters According to Scan Modes and Slice Thicknesses

	Image Acquisition Parameters	
Scan Parameters (slice thickness and scan mode)	Scan Time (seconds)	Number[a] of Reconstructed Slices
1.25 mm and Axial	43 [99][b]	172
1.25 mm and HQ	59 (3.75)[c]	171
1.25 mm and HS	30 (7.50)[c]	171
2.50 mm and Axial	21 [49][b]	84
2.50 mm and HQ	30 (7.50)[c]	86
2.50 mm and HS	16 (15.00)[c]	86
3.75 mm and Axial	15 [34][b]	56
3.75 mm and HQ	21 (11.25)[c]	58
3.75 mm and HS	16 (15.00)[c]	58
5.00 mm and Axial	11 [26][b]	44
5.00 mm and HQ	16 (15.00)[c]	43
5.00 mm and HS	8 (30.00)[c]	44

[a]Indicates the number of tomographic images reconstructed with acquisition slice thickness.

[b]Number in brackets indicates total scan time (seconds) including inter scan delay (ISD) time in the axial scan modes.

[c]Number in parentheses indicates table speed (mm per rotation) in the helical scan modes.

Table 3. Results of Twenty-one Items of Direct Distance Measurements on the Skull Specimen and Distance Measurements on 3D Rendered Images

		Direct Distance Measurements	Distance Measurements on 3D Rendered Image	
			1.25-mm Slice Thickness in Axial Scan Mode	5.00-mm Slice Thickness in Axial Scan Mode
No.	Abbreviation	Mean ± SD[a] (mm) (CV[b])	Mean ± SD[a] (mm) (CV[b])	Mean ± SD[a] (mm) (CV[b])
1	N-Ba	99.30 ± 0.27, (0.28)	101.00 ± 0.33, (0.32)	101.75 ± 0.31, (0.30)
2	N-Me	115.54 ± 0.21, (0.18)	115.12 ± 0.45, (0.39)	115.99 ± 0.44, (0.38)
3	N-Ans	50.40 ± 0.22, (0.44)	50.02 ± 0.63, (1.26)	47.93 ± 0.37, (0.76)
4	Ans-Me	66.52 ± 0.23, (0.34)	66.19 ± 0.29, (0.44)	68.71 ± 0.26, (0.38)
5	Ans-Pns	49.70 ± 0.07, (0.14)	48.80 ± 0.39, (0.79)	47.20 ± 0.30, (0.32)
6	Co(rt)-Pog	112.96 ± 0.29, (0.26)	111.90 ± 0.69, (0.61)	109.57 ± 0.35, (0.32)
7	Co(lt)-Pog	115.14 ± 0.17, (0.15)	114.88 ± 0.75, (0.65)	113.36 ± 0.49, (0.44)
8	N-Go(rt)	122.04 ± 0.23, (0.19)	121.97 ± 0.47, (0.39)	123.39 ± 0.34, (0.27)
9	N-Go(lt)	120.48 ± 0.13, (0.11)	120.81 ± 0.60, (0.50)	123.32 ± 0.45, (0.37)
10	A-B	36.16 ± 0.21, (0.57)	37.03 ± 0.63, (1.69)	36.56 ± 1.08, (2.97)
11	B-Me	22.65 ± 0.12, (0.53)	22.44 ± 0.62, (2.74)	23.30 ± 0.82, (3.54)
12	Go(rt)-Me	83.48 ± 0.21, (0.26)	84.19 ± 1.01, (1.20)	81.31 ± 0.50, (0.62)
13	Go(lt)-Me	85.89 ± 0.12, (0.14)	86.42 ± 0.95, (1.10)	83.05 ± 0.53, (0.64)
14	Co(rt)-Go	50.71 ± 0.08, (0.16)	48.60 ± 0.75, (1.54)	50.97 ± 0.68, (1.33)
15	Co(lt)-Go	50.76 ± 0.18, (0.36)	50.00 ± 0.71, (1.43)	53.86 ± 0.72, (1.33)
16	Co(rt)-Me	114.15 ± 0.38, (0.33)	112.53 ± 0.64, (0.57)	111.06 ± 0.71, (0.64)
17	Co(lt)-Me	116.53 ± 0.20, (0.18)	115.80 ± 0.59, (0.51)	116.47 ± 0.38, (0.33)
18	Zm-Zm	92.02 ± 0.13, (0.14)	93.05 ± 0.75, (0.81)	94.77 ± 0.42, (0.45)
19	Go-Go	94.81 ± 0.22, (0.23)	94.32 ± 0.96, (1.02)	94.19 ± 0.64, (0.68)
20	Or-Or	60.33 ± 0.13, (0.22)	60.75 ± 0.82, (1.34)	65.27 ± 0.29, (0.44)
21	Co-Co	118.00 ± 0.07, (0.06)	117.84 ± 0.43, (0.36)	117.98 ± 0.07, (0.06)

[a]SD: standard deviation.

[b]CV: coefficient of variance = 100% × standard deviation/mean.

comparatively analyzed with the corresponding data sets of MDCT measurements according to each scan mode and each slice thickness using two-way analysis of variance (ANOVA) and Tucky's studentized range test. In this study, *P* values less than .05 were regarded as indicating significant difference from the gold standards.

RESULTS

A radiologist measured the direct distances of 21 lines between 12 selected reference points on the skull surface five times for each item, with an accuracy of 0.01 mm (Table 3). The standard deviation of the direct measurements ranged from 0.07 mm for the Co-Co and Ans-Pns item to 0.38 mm for the Co(rt)-Me item, indicating the high level of consistency in the direct measurements. The direct distance measurements were therefore used as gold standards for quantitative analysis of the distance measurements on the 3D rendered images. The coefficients of variances (CV = 100% × standard deviation/mean) of the 21 direct measurement items ranged from 0.06% for the Co-Co item to 0.57% for the A-B item. These results show a high level of accuracy in the direct measurements, with an average CV of 0.25% (Table 3).

The frontal views of 3D rendered MDCT images of the skull specimen acquired according to the various scan modes and slice thicknesses are shown in Fig 3. Visual inspections indicated that the image quality of 3D rendered MDCT images was gradually degraded with increasing acquisition slice thickness and was not discriminated among the scan modes.

An observer also measured, seven times for each item, the 21 corresponding distance items on the 3D rendered MDCT images, which were displayed on a monitor according to scanning parameters. Figure 4 shows the means and standard deviations of the absolute difference between the distance measurements on 3D rendered images and the direct measurements for the 21 items acquired according to the 12 scanning parameters. The accuracy of distance measurement on the 3D rendered images was affected more by the acquisition slice thickness than the acquisition scan mode.

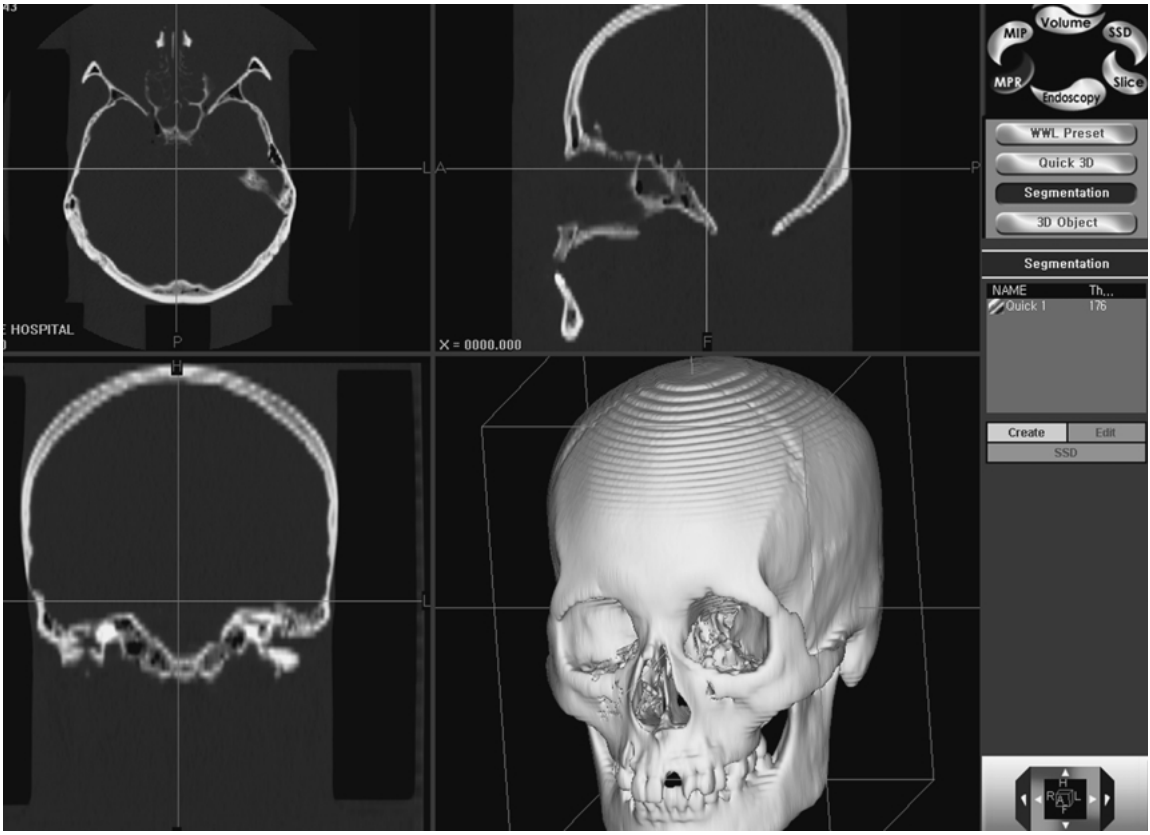

Fig 2. Distance measurements on 3D rendered images projected on a monitor.

Statistical evaluation of the distance measurements of 3D rendered images was performed using two-way ANOVA and Tukey's studentized range test for the 21 items, with each data set acquired at different slice thicknesses per scan mode. Statistical analysis for the quantitative accuracies of the distance measurements of 3D rendered images was performed according to 12 scanning parameters, scan mode, and acquisition slice thickness (Fig 5). The scan modes for each slice thickness were found to have no significant effect on distance measuring accuracy. The acquisition slice thickness for each scan mode was, however, an influential factor, with smaller thicknesses resulting in better accuracy.

DISCUSSION

Recent advances in CT technology have led to the development of MDCT, a modality that provides shorter image acquisition times, greater volume coverage, and higher longitudinal image resolution. Moreover, PACS implementation in the medical field provides easy access to the digital image data for various medical imaging modalities. Furthermore, the perspective views supplied by the 3D rendering technique can provide additional anatomic information and accurate physical measurements not available from 2D images. The use of 3D rendered images has therefore been increasing in medical applications.

Although 3D medical images are finding more and more applications, sufficient quantitative analysis of 3D rendered images has not been performed. Many studies have reported that scanning parameters, slice thickness, and scan mode influenced 2D tomographic image quality and accuracy in CT. We therefore performed quantitative analysis of the measurement accuracy of 3D rendered images, acquired according to various scanning parameters, by comparing the measured distances between di-

Fig 3. The frontal views of 3D rendered MDCT images of the skull specimen displayed according to scanning mode and slice thickness. A, axial 1.25 mm. B, high-quality 1.25 mm. C, high-speed 1.25 mm. D, axial 1.25 mm. E, high-quality, 1.25 mm. F, high-speed, 1.25 mm. G, axial, 1.25 mm. H, high-quality, 1.25 mm. I, high-speed, 1.25 mm. J, axial, 5.00 mm. K, high-quality, 5.00 mm. L, high-speed 5.00 mm. Figures show that the image quality of 3D rendered MDCT images gradually degraded with increasing acquisition slice thickness and was not discriminated among the scan modes. (Arrows indicate defects on the 3D rendered images.)

rect measurements on the skull and corresponding measurements on the 3D rendered image. We defined the means of direct measurements on the skull surface, which were conducted by a radiologist experienced in anatomic structures, as the reference gold standards. As one method of quantitative analysis of the 3D rendered images, we carried out a statistical analysis by evaluating the quantitative accuracies of distances measured on the 3D rendered image compared with the directly measured distances.

The average CV of the 21 direct measurement items was 0.25% (Table 3). Meanwhile, as an example of distance measurements on the 3D rendered images, the average CVs of distance

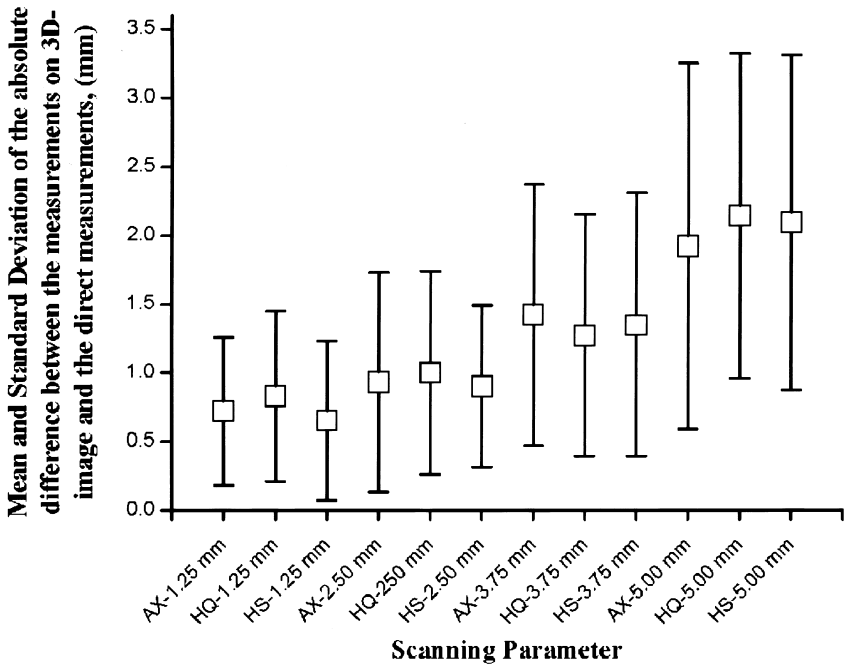

Fig 4. The means and standard deviations of the absolute difference between the distance measurements on 3D rendered images and the direct measurements, according to scanning parameters.

measurements on the 3D rendered images for 1.25, 2.50, 3.75, and 5.00 mm slice thicknesses in axial mode ranged from 0.74% to 0.94%. (For examples, only the 3D data for 1.25 mm and 5.00 mm slice thickness are listed in Table 3). The overall CVs of distance measurements on the 3D rendered images were three - to fourfold higher than CVs of the direct distance measurements. These results may be effectively used to predict the inaccuracy of distance measurements on 3D rendered images.

Intuitive visual inspections of the image quality of 3D rendered MDCT images indicated that defects in those images gradually increased with increasing acquisition slice thickness, but this degradation was not associated with any change in scanning mode (Fig 3). Figure 4 shows that the inaccuracy of distance measurements on 3D rendered images increased as acquisition slice thickness was increased, but it was also interpreted to be weakly affected by acquisition scan mode.

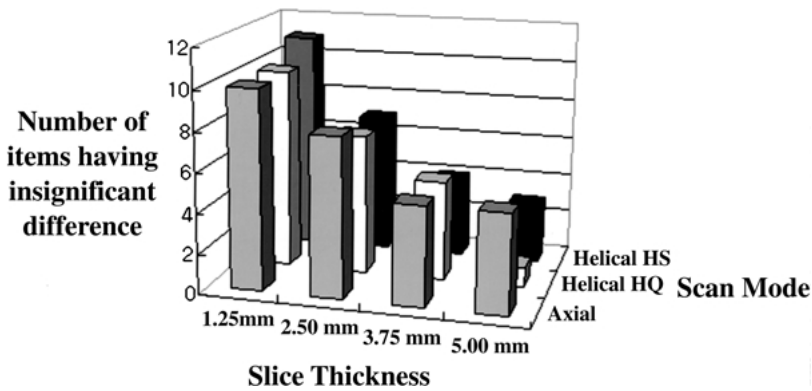

Fig 5. Number of items having insignificant difference ($P > .05$) among 21 distance measurement items according to 12 scanning parameters, obtained from comparative statistical analysis between direct measurements on the skull and distance measurements on 3D rendered MDCT images.

In general, the image quality of MDCT 2D tomographic images has been evaluated by visual observation analysis to be equal to or better in axial scan mode than in helical scan mode.[10] Meanwhile, the results of quantitative analysis of the 3D rendered images revealed that accuracy of distance measurements was not significantly different among the three scan modes for each slice thickness. As shown in Table 2, the total scan time for the same volume coverage was decreased in the order of axial, high quality (HQ), and high speed (HS) modes. Increasing scan time may lead to an increase in the amount of x-ray photons related to the radiation dose or to a degradation of image quality caused by motion artifacts.[4,16,17] Our results indicate that if quantitative accuracy is equal for medical applications with 3D rendered images, then the helical (HQ or HS) scan mode should be sufficiently efficient for head scan protocols with the associated benefits of shorter scan time and/or less radiation dose. Given these findings, the helical mode could substitute for the axial mode now in use in daily clinical practice.

CONCLUSIONS

In conclusion, the quantitative accuracy of distance measurements of 3D rendered images with MDCT was influenced by slice thickness rather than scan mode. The quantitative analysis of distance measurement may be a useful tool to for evaluating the accuracy of 3D rendered images helping in diagnosis, surgical planning, and radiotherapeutic treatment.

ACKNOWLEDGMENTS

This study was supported in part by the Brain Korea 21 Project for Medical Sciences, by the Research Institute of Radiological Science, Yonsei University, and by grant R01-2002-000-00205-02002 from the Basic Research Program of the Korea Science & Engineering Foundation. We thank Dong-Kee Kim and Min-Ji Kim, Department of Biostatistics, College of Medicine,Yonsei University, for their assistance with the statistical analysis and Kook-Jin Jeon, Department of Dental Radiology, College of Dentistry, Yonsei University, for her assistance with preparing the skull specimen and the direct measurements.

REFERENCES

1. Hu H: Multi-slice helical CT: scan and reconstruction. Med Phys 26:5-18, 1999
2. Hu H, He HD, Foley WD, et al: Four multidetector-row helical CT: image quality and volume coverage speed. Radiology 215:55-62, 2000
3. Wang GE, Vannier MW: The effect of pitch in multislice spiral/helical CT. Med Phys 26:2648-2653, 1999
4. McCollough CH, Zink F: Performance evaluation of a multi-slice CT system. Med Phys 26:2223-2230, 1999
5. Lee JS, Jani AB, Pelizzari CA, et al: Volumetric visualization of head and neck CT data for treatment planning. Int J Radiat Oncol Biol Phys 44:693-703, 1999
6. Verstreken K, Van Cleynenbreugel J, Marchal G, et al: An image-guided planning system for endosseous oral implants. IEEE Trans Med Imaging 717:842-852, 1998
7. Pretorius ES, Fishman EK: Volume-rendered three-dimensional spiral CT: musculo skeletal applications. Radiographics 19:1143-1160, 1999
8. Urban BA, Rantner LE, Fishman EK: Three-dimensional volume-rendered CT angiography of the renal arteries and veins: normal anatomy, variants, and clinical applications. Radiographics 21:373-386, 2001
9. Lawer LP, Fishman EK: Multi-detector row CT of thoracic disease with emphasis on 3D volume rendering and CT angiography. Radiographics 21:1257-1273, 2001
10. Honda O, Johkoh T, Tomiyama N, et al: High-resolution CT using multidetector CT equipment: evaluation of imaging quality in 11 cadaveric lungs and a phantom. AJR Am J Roentgenol 177:875-879, 2001
11. Nikolaou K, Huber A, Scheidler J, et al: Navigator echo-based respiratory gating for three-dimensional MR coronary angiography: reduction of scan time using a slice interpolation technique. J Comput Assist Tomogr 25:378-387, 2001
12. Zeiberg AS, Silverman PM, Sessions RB, et al: Helical (spiral) CT of the upper airway with three-dimensional imaging: technique and clinical assessment. AJR Am J Roentgenol 166:293-299, 1996
13. Nagashima M, Inoue K, Sasaki T, et al: Three-dimensional imaging and osteometry of adult human skulls using helical computed tomography. Surg Radiol Anat 20:291-297, 1998
14. Cavalcanti MGP, Vannier MW: Quantitative analysis of spiral computed tomography for craniofacial clinical applications. Dent Maxillofac Radiol 27:344-350, 1998
15. Cavalcanti GP, Haller JW, Vannier MW: Three-dimensional computed tomography landmark measurement in craniofacial surgical planning : experimental validation in vitro. J Oral Maxillofac Surg 57:690-694, 1999
16. Mukherji SK, Castillo M, Huda W, et al: Comparison of dynamic and spiral CT for imaging the glottic larynx. Comput Assist Tomogr 19:899-904, 1996
17. Engeler CE, Tashjian JH, Engeler CM, et al: Volumetric high-resolution CT in the diagnosis of interstitial lung disease and bronchiectasis: diagnostic accuracy and radiation dose. AJR Am J Roentgenol 163:31-35, 1994